Available online at www.sciencedirect.com

ScienceDirect

Physics Procedia 5 (2010) 551–560

Physics Procedia

www.elsevier.com/locate/procedia

LANE 2010

Selective laser melting technology: from the single laser melted track stability to 3D parts of complex shape

I. Yadroitsev*, I. Smurov

Ecole Nationale d'Ingénieurs de Saint-Etienne (ENISE), DIPI Laboratory, 58 rue Jean Parot, 42023 Saint-Etienne Cedex 2, France

Abstract

To up-grade SLM process for manufacturing real components, high mechanical properties of final product must be achieved. The properties of a part produced by SLM technology depend strongly on the properties of each single track and each single layer. In this study, effects of the processing parameters such as laser power, scanning speed and powder layer thickness on the single tracks formation are analyzed. It is shown that, by choosing an optimal technological window and appropriate strategy of SLM, it is possible to manufacture highly complex parts with mechanical properties comparable to those of wrought material.

Keywords: Rapid manufacturing; Selective laser melting; Metal powders

1. Introduction

Selective laser melting (SLM) is known as a unique technology to produce objects from metal powders with complex geometry and mechanical properties comparable to those of bulk materials. Also, it is a promising method for fabrication of functionally graded multi-material parts. SLM technology can be used at all the stages of the product development – from design concept to low volume production [1, 2].

Selective laser melting comprises the following physical phenomena: absorption and scattering of laser radiation, heat transfer, phase transformation, fluid flow within the molten pool caused by surface-tension gradient, evaporation and emission of material, and chemical reactions. The SLM process is also defined by a large number of parameters including the processing parameters such as laser power, scanning speed, scan line spacing (hatch distance), thickness of layer, scanning strategy, working atmosphere, temperature of powder bed, and material-based input parameters. All of them have an effect on the process of the tracks formation. Unfortunately, their mutual interaction is not always clear. That is why very important scientific understanding of modification of processing parameters, i.e. how the modification each of these parameters influences on the other and the SLM process as a whole.

* Corresponding author. Tel.: +33-4-77437578; fax: +33-4-7774-3497.
E-mail address: yadroitsev@enise.fr.

1875-3892
doi:10.1016/j.phpro.2010.08.083

Volume fraction of the gases in the powder layer decreases from a high value upon starting to nearly zero after selective laser melting and significant density change occurs caused by melting [3]. The nature of the effective heat source produced by laser irradiation of a powder layer considerably differs from the case of laser irradiation of an opaque metallic body. Under laser irradiation of the surface of an opaque metallic body, the influence of the material properties on the energy balance can be described as the relationship between the material heat conductivity and the absorptivity: k/A. The absorptivity of a powder layer depends not only on the physicochemical properties of the powder material, but also on granulomorphometry and apparent density of the powder, and substantially higher than that of the bulk materials (e.g. $A_{\text{Cu bulk}}$=0.02, $A_{\text{Fe bulk}}$=0.36 and $A_{\text{Cu powder}}$= 0.6, $A_{\text{Fe powder}}$ =0.7 for λ=1.06 μm). Therefore, at the initial stage of SLM when powder is still in the solid state, the material properties influence the process mainly by thermal conductivity k; further on, when the powder is remelted, the k/A ratio should be taken into account. During laser treatment, only a part of radiation is absorbed by the particles at the outer surface of the loose powder layer. The rest of the radiation penetrates through the pores containing gases and interacts with the underlying particles. Further, the heat distribution into the powder layer is done by the usual heat transfer mechanisms. The intensity of the laser radiation decreases with its penetration into the powder layer [4-7].

The essential operation at SLM is the laser beam scanning over the surface of a thin powder layer previously deposited on a substrate or previously remelted layer, which is a substrate for the following layer. Each cross-section (layer) of the part is sequentially filled with elongated tracks of melted powder. Line-by-line, a laser beam melts the material along a row of powder particles, thereby forming a molten pool. Under the effect of surface tension, the molten pool takes the shape of a circular or segmental cylinder. Fragmentation of the remelted tracks is a well-known drawback of SLM referred to as the "balling" effect [7-8]. The features of the tracks' instability depend of laser power, scanning speed, powder layer thickness, substrate material, physical properties and granulomorphometry of the powder used [9-14]. The properties of a part produced by SLM technology depend strongly on the properties of each single track and each single layer. In order to use a wider range of commercially available powders, an in-depth study of the mechanisms of formation of single laser-melted tracks and of the instabilities of the molten pool is required. In this paper, the capillary instability of segmental cylinders and effects of the processing parameters such as scanning speed, laser power and powder layer thickness on the single tracks formation (technological processing map, geometric characteristics) are analyzed.

2. Materials and experimental procedure

The experiments were carried out on SLM machine PM 100 (Phenix Systems). The source of radiation is YLR-50 cw Ytterbium fiber laser by IPG Photonics operating at the wavelength of 1075 nm. The main characteristics of the PM 100 machine are as follows: the maximum laser power is P=50 W, the maximum laser scanning speed is V=3 m/s, the laser spot size is 70 μm, the minimum layer thickness is 5 μm (for fine powders). The furnace of the machine provides a temperature up to 900°C and has a closed environment filled by nitrogen or argon as a protective gas. The operational temperature of the internal chamber was fixed at 80ºC.

Table 1. Powder characteristics

Materials / Powder characteristics		316L (–25 μm)	904L (–16 μm)	CuNi10 (–25 μm)	H13 (–25 μm)	Inconel 625 (–16 μm)	Co212-F (–31 μm)
Equivalent diameter (weight by volume), μm	p_{10}	5.3	5.1	6.8	8.8	4.7	6.7
	p_{50}	14.5	11.2	17.5	12.9	9.0	16.7
	p_{90}	25.2	18.5	30.2	28.8	14.5	26.6
Volume specific surface, μm^{-1}		0.574	0.684	0.467	0.401	0.783	0.482
Apparent density, %		58±0.3	44±0.7	54±0.7	57±0.1	47±0.6	61±0.4
Tapped density, %		64±0.7	52±1.3	60±0.02	62±0.4	53±0.7	66±0.4

p_{10}-p_{50}-p_{90} are 10th, 50th and 90th percentiles of the studied indexes. 10-50-90 percentiles are the values below which 10-50-90% of the observations may be found.

The applied materials are pre-alloyed gas-atomized powders: SS grade 316L (–25 μm), CuNi10 (–25 μm), tool steel H13 (–25 μm) from TLS Technik GmbH & Co and SS grade 904L (–16 μm), Inconel 625 (–16 μm), Co212-F (–31 μm) from Sandvik Osprey Ltd. Granulomorphological analysis of the particles was carried out by the optical granulomorphometer ALPAGA 500 NANO (OCCHIO s.a.) which is a real-time optical sieving system. The equivalent diameters (weight by volume), volume specific surface, tapped and apparent densities of the employed metal powders are present in Table 1. For all the powders, most of the particles had a high sphericity and a smooth surface with a negligible quantity of satellites.

3. Experimental results and discussion

3.1. Single track formation from SS grade 904L powder

The formation of the first-layer single tracks is a focus of this study. The tracks of SS grade 904L powder on a SS grade 304L substrate were produced by the 50 W and 25 W power laser beam at different scanning speeds ranging from 0.06 to 0.24 m/s and 0.03 to 0.12 m/s correspondingly. The thickness of the deposited powder layer was 50 μm. The length of the scan line was 20 mm for all the experiments. The width of the tracks, the zone of powder consolidation and the remelted depth (penetration into substrate) were analyzed (Fig. 1).

It was found that the width of the single track varied from 130 to 100 μm, the width of the zone of powder consolidation varied from 260 to 130 μm. The track width and the zone of powder consolidation decreased with the scanning speed (Fig. 2).

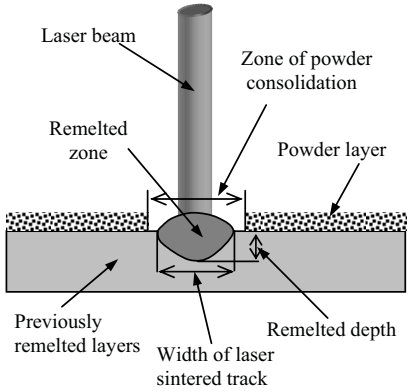

Fig. 1. Typical cross-section of a laser sintered track from metal powder on steel substrate

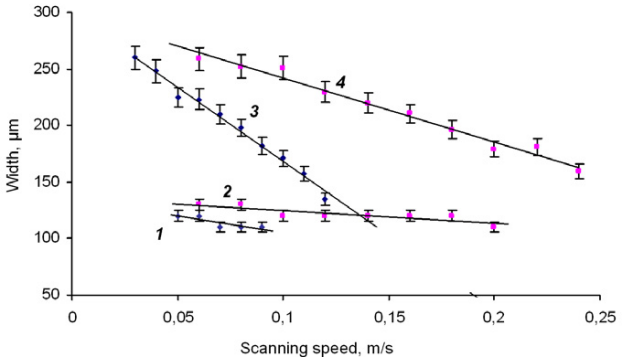

Fig. 2. The width of the single tracks (curves 1-2) from SS grade 904L and the width of the zone of powder consolidation (curves 3-4) versus scanning speed of the laser beam for different power. Thickness of the deposited powder layer is 50 μm, $V = 0.03–0.24$ m/s for $P = 25$ W (curves 1, 3) and 50 W (curves 2, 4)

For the laser power P=25 W, the substrate remelted depth is absent for all the range of the scanning speeds used, i.e. the laser power is sufficient to melt the powder but, under the given process parameters, is not enough to melt the substrate and to create a joint molten pool. The molten powder forms a rounded free surface (circular cylinder) and has a very small contact zone with the substrate. The thermo-physical conditions of the tracks sintering change: the indirect interaction by the heat conductivity of the substrate and the convection phenomena decreases, and, therefore, the amount of powder involved in the process of track formation diminishes, and the penetration into the substrate is almost absent. The existence of the stability and instability zones must be noted: the former ones are characterized by the formation of a stable molten pool and continuous tracks, the latter ones are presented by non-continuous tracks and the drops formation [7]. For SS grade 904L (–16 μm) powder stable zones of the single tracks are formed at a scanning speed from 0.06 to 0.09 m/s at the laser power 25 W and from 0.06 to 0.18 m/s at P=50 W.

At the laser power of 50 W, non-continuous single tracks occur at the scanning speed of 0.20 m/s and higher. At P=25 W, broken single tracks are formed at the scanning speeds under 0.06 m/s, while at the speeds above 0.09 m/s the drops formation starts abruptly.

At a low scanning speed and the absence of the remelted depth (laser power 25 W, scanning speed less than 0.06 m/s), the heat sink into the substrate diminishes, the molten pool overheating occurs, and the tracks become unstable and irregular. At 50 W laser power, the contact zone between the remelted powder and the substrate tends to vanish at the scanning speed $V > 0.20$ m/s.

The remelted depth decreases with the scanning speed, the shape of the liquid pool is significantly affected [15-17]. The molten free circular cylinder breaks into two droplets if its length exceeds its circumference (limit of the Plateau-Rayleigh capillary instability for a liquid cylinder [18]).

3.2. Instability of the molten pool at low scanning speed

The instability of the molten pool at low scanning speed was studied by the example of SS grade 316L (–25 μm) powder. The tracks were formed by the 12.5 ÷ 50 W power laser beam at different scanning speeds ranging from 0.02 to 0.22 m/s with a step of 0.04 m/s, the powder layer thickness was 50 μm. Three tracks were produced for each set of input parameters P and V. For the given laser power, the temperature and volume of the molten powder are higher at lower scanning speeds. With the increase of the energy input per unit length (P/V) at a relativity high laser power and a small scanning speed, SLM process is accompanied by an increase of the melt volume and a decrease of the melt viscosity. The melt hydrodynamics (driven by Marangony effect [19-22]) becomes increasingly important, and the irregularity of the sintered track appears.

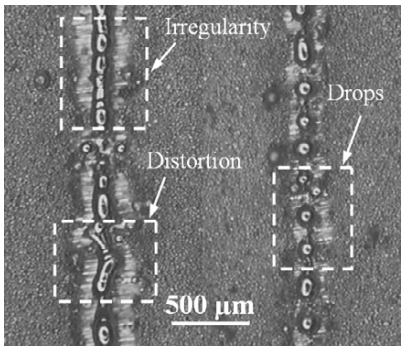

(a) (b)

Fig. 3. Instability of laser sintered tracks from SS grade 316L (–25 μm) powder on steel substrate. The layer thickness is 50 μm, V = 0.02 m/s: (a) P =25 W, (b) P =12.5 W

For SS grade 316L (4×10^{-6} m^2/s thermal diffusivity) with 25 μm grain diameter, the entire grain becomes uniformly heated after about 40 μs irradiation time [23]. At 70 μm spot diameter and 0.03-0.06 m/s scanning speed, the laser irradiation time is 2.3-1.1 ms. So, in this case, the already melted powder is exposed during most of the laser irradiation time. At smaller laser power for small scanning speed, the energy becomes insufficient to melt the substrate, and the stabilizing effect of the contact zone (penetration into substrate) disappears. If the energy is enough to maintain the boiling and evaporation of the molten powder, the vapour recoil pressure causes distortion and irregularity of the sintered tracks (Fig. 3a). With the further reduction of the laser power, the tracks become a sequence of drops (Fig. 3b).

3.3. Influence of the powder layer thickness on the single track formation

Since SLM is a layer-by-layer technique, the layer thickness is one of the determinant factors of this process. The appropriate choice of the layer thickness should be based on a thorough consideration of the particle size and the shrinkage extent during synthesis. The thickness of a deposited layer determines how much powder will be melted by a single laser scan. Single tracks from SS grade 316L (–25 μm) powder were formed on metal substrate (SS grade 304L); the layer thickness smoothly varied from 0 up to 400 μm. For the maximum laser power of 50 W, the scanning speed ranged from 0.04 to 0.28 m/s with a step of 0.02 m/s (Fig. 4), for 25 W laser power – from 0.02 to 0.14 m/s with a step of 0.01 m/s.

At the layer thickness less than 50 μm, practically all the SS grade 316L (–25 μm) particles interacted with the laser radiation within the laser spot. If the optimum energy balance is achieved, a continuous laser melted track may be obtained. An excessive energy causes distortion and irregularity (Fig. 3). For example, at P=50 W, irregular tracks were sintered at low scanning speed – 0.04 and 0.06 m/s – for the layer thickness 40–120 μm and 40–90 μm, respectively. The minimal and maximal layer thickness (critical thickness) allowing to produce continuous single

melted tracks from SS grade 316L (-25 μm) powder at 50 W laser power are presented in Fig. 4. For 0.04 m/s scanning speed, the critical thickness is 0–40 μm and 120–300 μm. For P = 25 W and 0.02 m/s scanning speed, it is 0–40 μm and 180–210 μm. The maximal layer thickness for producing continuous single tracks increases with the energy input. A higher power is more preferable as it gives a greater degree of freedom for variation of the scanning speed and the thickness of the powder layer.

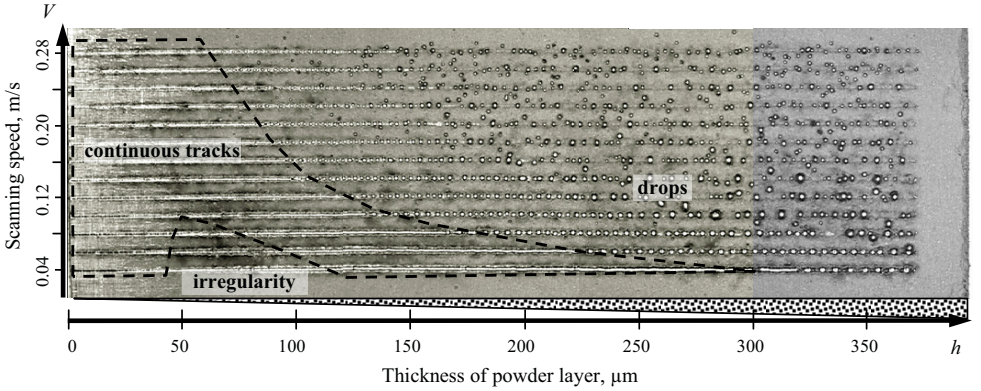

Fig. 4. Top view of laser sintered tracks from SS grade 316L (–25 μm) powder on steel substrate. Thickness of the deposited powder layer h varies in the range 0÷400 μm, laser power is 50 W, scanning speed is V = 0.04÷ 0.28 m/s

3.4. Optimal scanning parameters for different metal powders

For 50 μm thickness of the deposited powder layer and 50 W laser power continuous single tracks from SS grade 316L (–25 μm) can be formed at V=0.08–0.20 m/s scanning speed, and from SS grade 904L (–16 μm) at V=0.06–0.18 m/s scanning speed. Also, for P=25 W, continuous tracks from 904L powder were formed at a lower scanning speed (0.06–0.09 m/s) compared to 316L (0.10–0.12 m/s). For stainless steels grade 904L and 316L, the thermal conductivity is k=12.5 $W \cdot m^{-1} \cdot K^{-1}$ and 16.2 $W \cdot m^{-1} \cdot K^{-1}$, the specific heat capacity is c_p=439–450 $J \cdot kg^{-1} \cdot K^{-1}$ and 500–530 $J \cdot kg^{-1} \cdot K^{-1}$, the thermal diffusivity is α=3.42·10^{-6} m^2/s and 4.1·10^{-6} m^2/s, the melting point is T_m =1315–1390°C and 1375–1400°C, respectively [24]. The latent heat of fusion influences the heat balance [25-27], and SS grade 904L has a higher latent heat of fusion: 500 kJ/kg versus 275 kJ/kg for SS grade 316L. That is why continuous tracks from SS grade 904L are formed at a lower scanning speed compared to 316L. The process map obtained for SS grade 316L powder for thickness of layer about 50 μm is presented in Fig. 5. The range of admissible scanning speed is larger for the higher laser power. Rehme and Emmelmann [28] indicate the scanning speed V=0.10 m/s as a typical value for processing SS grade 316L (–20 μm) at layer thickness 20–50 μm and the laser power P=100 W.

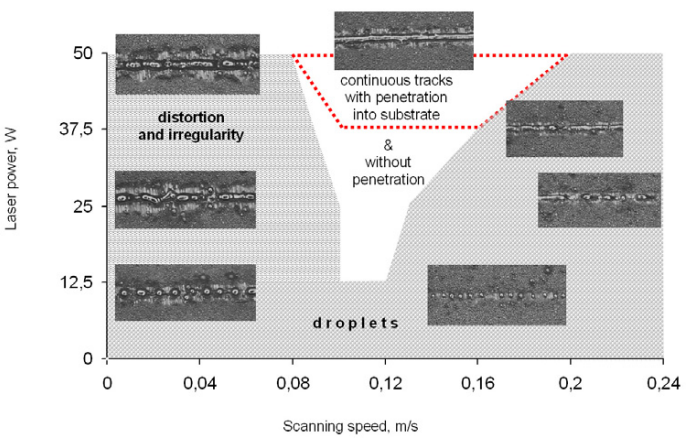

Fig. 5. Single track process map for the first layer of SS grade 316L (–25 μm) powder. Powder layer thickness is 50 μm

Under SLM conditions a set of

phenomena (heat conduction, melting, densification, cooling) takes place simultaneously within a short time. Naturally, different materials demonstrate different behaviour induced by the above phenomena [28-30]. The interaction of two dissimilar metals with the different thermo-physical properties was studied by forming single tracks from CuNi10 powder on SS grade 304L substrate.

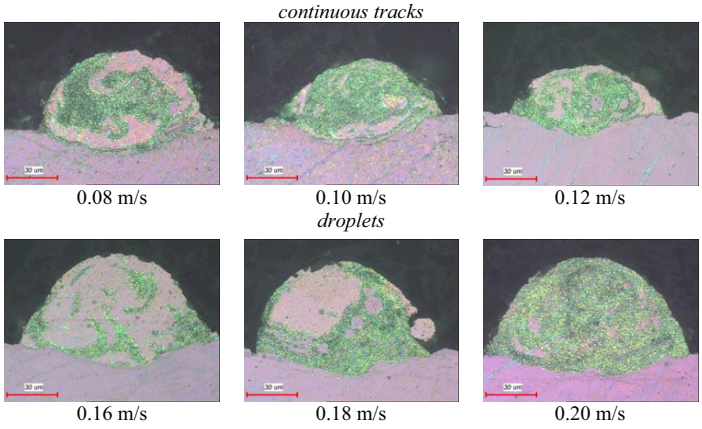

Fig. 6. Cross-sections of laser sintered tracks from CuNi10 (–25 μm) powder on SS grade 304L substrate. Thickness of the deposited powder layer is 50 μm, laser power 50 W, scanning speed V =0.08–0.20 m/s

The width of the CuNi10 single tracks was 140 μm for V=0.08 m/s scanning speed, and it was about 90 μm for V=0.14 m/s at 50 W laser power. The substrate remelted depth was practically constant (about 15 μm) at 0.08–0.20 m/s scanning speed (Fig. 6). The balling effect was observed starting from 0.15 m/s scanning speed. At 25 W laser power and 0.06–0.12 m/s scanning speed, the track width is significantly smaller (65–50 μm) compared to SS grade 904L (120–100 μm), and it quickly decreases with the energy input. The balling effect was observed for the whole range of scanning speeds 0.06–0.22 m/s, and the substrate remelted depth was absent. The copper alloys have a considerably lower melting point compared to SS grade 304L and a lower radiation absorptivity A at λ = 1.06 μm (A_{Cu} = 0.02-0.2 vs A_{Fe} = 0.36). CuNi10 has a higher thermal conductivity by 2.6 times greater (42.5 $Wm^{-1}K^{-1}$ versus 16.2 $Wm^{-1}K^{-1}$). The copper-nickel alloy has a lower surface tension compared to SS grade 304L (~1.2 N/m and ~1.9 N/m, respectively) [24]. A good wettability of the substrate and a wide zone of contact induce an intensive heat transfer. The temperature gradients will generate coupled heat- and mass-transfer processes. Besides, the density gradient is created in the molten pool not only by the temperature heterogeneity but also by the fluctuation of concentration. In Fig. 6 vortexes are well visible as a result of convection currents. It is known that the convection processes are closely connected to the instability that limits the range of optimal processes parameters for the formation of continuous tracks from the CuNi10 alloy.

Optimal scanning speeds were found at P=50 W laser power for the formation of continuous single tracks on substrate from the deposited 50 μm-thick powder layer of SS grade 904L, 316L, tool steel H13, copper alloy CuNi10, superalloy Inconel 625. With the increase of the thermal conductivity of the bulk materials, the range of optimum scanning speeds narrows, the correlation coefficient between the thermal conductivity of the bulk materials and the range of optimal scanning speeds equals –0.95 (p–level 0.01).

3.5. Mechanical properties of the manufactured samples

The mechanical properties of SLM parts are anticipated to be anisotropic mainly due to the fact that the part build-up is conducted with many layers melted onto each other and are determined by the solidification microstructure, while the solidification microstructure essentially depends on the local solidification. Density is a crucial factor for strength in SLM parts. Special strategies have been employed to achieve the maximum density of the samples (less than 1% porosity), so-called “two-zone” and “cross-hatching” techniques. The notion of “two-zone” implies that each powder layer is processed by the laser beam twice. Firstly, the layer is processed with a hatch distance equal to the width of the laser remelted track for a given powder (e.g. 120 μm for SS grade 316L (–25 μm) powder), then the laser beam passes in between the remelted tracks of the same layer thus melting no powder but two neighbouring tracks. The cross-hatching means the scanning of the successive layer perpendicular to the previous one. A key point of this technique is to avoid the formation of periodic wave structure which otherwise accumulates with each newly synthesized layer. Research has shown that once a pore has formed, it can propagate

itself through subsequent layers forming an interconnected void. So, cross-hatching helps to avoid the formation of the interconnected porosity [31]. It is well known that, in powder metallurgy (PM) of steels, porosity is detrimental to the mechanical properties. The pores act as stress concentrators leading to an earlier onset of plasticity and localization of strain. Both morphology and distribution of pores have a significant effect on the mechanical behavior of PM steels. The more irregular the pores or the higher the degree of pore clustering, the lower is the ductility [32].

A series of three samples were synthesized from SS grade 316L (–25 μm) and Co212-F (–31 μm) by combining the two-zone and cross-hatching techniques using the following parameters: 50 W laser power, 40 μm layer thickness, 0.12 m/s scanning speed, 120 μm hatch distance. Rounded specimens according to ISO-7500/1 were fabricated and mechanically tested. Some of their mechanical properties are shown in Table 2.

Table 2. Results of the tensile testing at room temperature of SLM samples manufactured from SS grade 316L (–25 μm) and Co212F (–31 μm)

Materials / Mechanical properties	SS grade 316L		CoCr alloy	
	SLM	Wrought [33]	SLM	Wrought [33]
Ultimate tensile strength, MPa	436±60	480-560	980±30	720–1000
Yield strength (0.2% offset), MPa	366±50	170-290	817±20	565–650
Elongation, %	9±2	~40	8±2	9–20
Young's modulus, GPa	179±3	190-210	-	-
Poisson's ratio	0.30	0.27-0.30	-	-

To study mechanical properties of SLM parts from Inconel 625 (–16 μm) powder, rectangular samples 50x20x4 mm were fabricated by two-zones technique, with the laser power 50 W, the layer thickness 50 μm, and the scanning speed 0.13 m/s. The samples were built on the substrate at angles of 0°, 90° and 45° to the scanning direction which remained the same through the manufacturing cycle. The fabricated samples were «horizontal» or «vertical»: the first ones were rectangular parallelepipeds with their long surfaces coinciding with the laser scanning plane (50 mm length and 20 mm height) and the second ones stood up on their short 20x4 mm surfaces (50 mm height). Specially shaped models were made from the samples for tensile tests. The tensile tests showed that inside each series of samples – «horizontal» and «vertical», 3 samples in each series, the mechanical properties were approximately identical and did not depend on the scanning strategy (see Tables 3 and 4). It is necessary to note that the samples manufactured by SLM technology have higher values of yield strength and ultimate tensile strength in comparison with the ones from wrought Inconel 625 that is probably linked to the presence of a regular internal structure of the samples [34]. The yield strength for «vertical» and «horizontal» samples almost equal, which indicates that the interface between two consecutive layers is not weakest joint [35]. However, elongation was only ~8÷10% compared to 40% for conventionally cast and wrought products. Similar results were obtained by Lewis et al. for Ti6Al4V (~6% elongation) [36]. The values of their relative elongation at break allow to relate them to materials with the limited plasticity. The average value of Young's modulus for the «horizontal» samples happened to be much higher than that for the «vertical» ones, and was approximately equal to Young's modulus of wrought Inconel 625 (207 GPa) [37].

Table 3. Tensile testing results at room temperature for wrought Inconel 625 and the samples manufactured by SLM method

Mechanical properties / Type	Ultimate tensile strength, MPa	Yield strength (0.2% offset), MPa	Elongation, %
Horizontal samples	1030±50	800±20	~ 8-10
Vertical samples	1070±60	720±30	~ 8-10
Wrought Inconel 625 [33]	940	430-520	~ 40

Table 4. Young's modulus values (GPa) for different manufacturing strategies and types of the samples from Inconel 625 powder

Strategy / Type	0°, GPa	90°, GPa	45°, GPa
Horizontal samples	206.34	206.88	199.49
Vertical samples	132.21	140.22	149.55

The «vertical» samples have numerous defects caused by a considerable amount of thermal stress accumulated during the heating/cooling cycles [10, 38-39] that correspond to a greater, compared to the «horizontal» samples, number of layers. As a result, they have lower values of Young's modulus. At the same time, the ultimate tensile strength has small dependence from the initial density of defects within the sample, because, at this value of the tensile strength, the density of dislocations becomes very high due to the deformation strengthening with no regard to the initial density of defects [34].

The fracture surfaces were analyzed using scanning electron microscopy (SEM) to identify the crack propagation modes. Some «horizontal» samples with scanning direction 0° have a monolithic structure with relatively small amount of defects (Fig. 7(a)). These defects could be classified like porous. Analysis of the destruction fractographs for monolithic area (Fig. 7(b)) shows combination of brittle and ductile fractures. Cleavage shows up clearly in the SEM. The higher value of the modulus of elasticity for the «horizontal» type of samples confirms that ductile fracture is the predominant destruction mechanism.

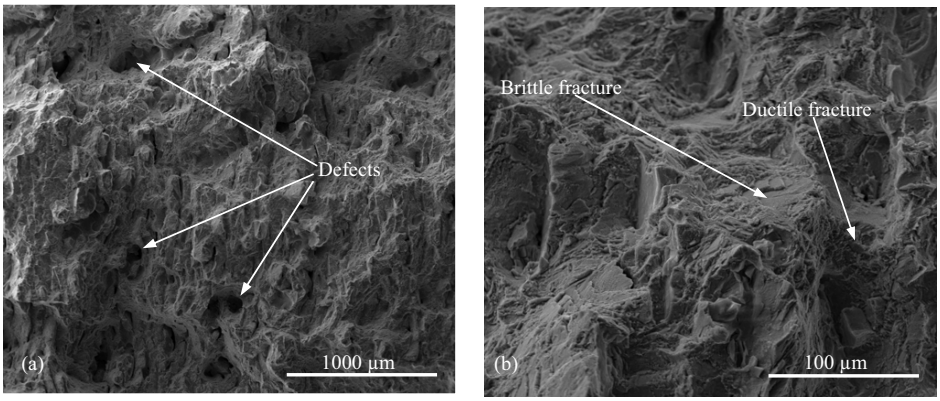

Fig. 7. SEM photo of a fracture surface morphology (a) and destruction for monolithic area (b) of the «horizontal» sample with scanning direction 0°

It is necessary to note that the samples manufactured by SLM (two-zone technique) have a greater elasticity within one layer than between layers. All the «vertical» samples broke at the layer contacts. The «horizontal» ones broke at the plane perpendicular to the laser scanning direction [30].

The analysis of the mechanical properties of the samples manufactured by SLM technique from Inconel 625, SS grade 316L and Co212-F powder has shown their excellent mechanical strength equivalent to the wrought materials. Based on the obtained results, several 3D models and functional prototypes with a complex geometry were fabricated from metal powders for different industrial applications: from aerospace and automotive to biomedical and chemical (Fig. 8).

4. Conclusion

The analysis of the formation of single tracks from metal powders by SLM showed that the process has a threshold character: there are "stability zones" where the laser melted track is continuous and "instability zones"

where the tracks are not continuous. Instabilities appear at low scanning speed in the form of distortions and irregularities, and, on the contrary, excessively high speed gives rise to the balling effect. The range of the optimal scanning speed is larger for the higher laser power, and it narrows for material with high thermal conductivity. The penetration into the substrate provides an additional stabilizing effect for the sintering of the continuous individual tracks. The influence of the processing parameters and manufacturing strategies on the mechanical properties of the fabricated objects was analyzed. Near full-density samples with the mechanical strength equivalent to the wrought material were produced from Inconel 625 (–16 μm), stainless steel grade 316L (–25 μm) and cobalt-chromium (–31 μm) powders by "two-zone" and "two-zone cross-hatching" technique. An effect of anisotropy of the mechanical properties was studied regarding the scanning directions. "Horizontal" and "vertical" samples were fabricated from Inconel 625 powder. The Young's modulus value for the "horizontal" samples is by 1.5 times higher than that for the "vertical" samples and is close to that of wrought Inconel 625. It was not found essential differences in the yield strength and ultimate tensile strength values for the ''vertical'' and ''horizontal'' samples depending to the scanning direction – 0°, 90° or 45°. The samples manufactured by "two-zone" technique have a greater elasticity within one layer than between layers.

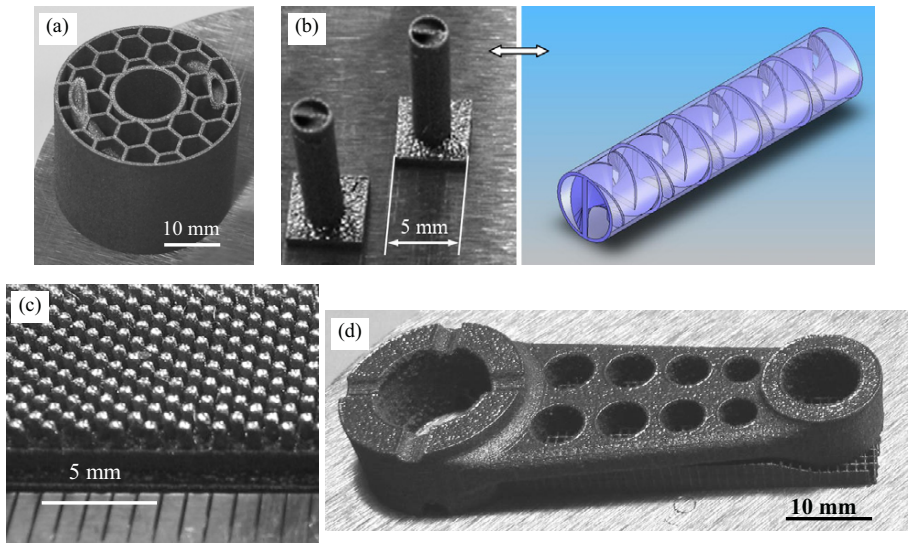

Fig. 8. 3D models and functional prototypes with a complex geometry fabricated by SLM: (a) light-weight model with complex inner structure and two spiral cooling channels from SS grade 316L powder; (b) mixing element Kenics with diameter 3 mm and height 15 mm and (c) sample with developed structure (pin diameter is 400 μm, height is 1 mm) from SS grade 904L powder; (d) part of combustion engine from Inconel 625 powder

References

1. P. J. S.Bartolo, H. A. Almeida, , N. F. Alves (eds.), Virtual and rapid manufacturing, Taylor & Francis Group, London, 2008.
2. T. Wohlers, State of the industry, annual worldwide progress report, Wohlers Associates, Inc., 2008.
3. Y. Zhang, A. Faghri, Int. J. Heat. Mass. Tran. 42 (1999) 775.
4. P. Fischer, N. Karapatis, V. Romano, R. Glardon, H. P. Weber, Appl. Phys. Mater. Sci. Process. 74 (4) (2002) 467.
5. P. Fischer, V. Romano, H. P. Weber, N. P. Karapatis, E. Boillat, R. Glardon, Acta Materialia. 51 (2003) 1651.
6. N. K. Tolochko, T. Laoui, Y. V. Khlopkov, S. E. Mozzharov, V. I. Titov, M. B. Ignatiev, Rapid Prototyping Journal 6 (3) (2000) 155.
7. N. K. Tolochko, S. E. Mozzharov, I. A. Yadroitsev, T. Laoui, L. Froyen, V. I. Titov et al., Rapid Prototyping Journal 10 (2) (2004) 78.

8. R. Morgan, C. J. Sutcliffe, W. O'Neill, Rapid Prototyping Journal 7 (3) (2001) 159.
9. P. Karapatis, A sub-process approach of selective laser sintering. PhD thesis, EPFL, LGPP, Lausanne, Switzerland, 2002.
10. J. P. Kruth, L. Froyen, J. Van Vaerenbergh, P. Mercelis, M. Rombouts, B. Lauwers, J. Mater. Process. Tech. 149 (2004) 616.
11. A. Simchi, Metall. Mater. Trans. B Process. Metall. Mater. Process. Sci. 35 (5) (2004) 937.
12. A. Simchi, Mater. Sci. Eng. 428 (2006) 148.
13. I. Yadroitsev, Ph. Bertrand, I. Smurov, Appl. Surf. Sci. 253 (2007), 8064.
14. K. A. Mumtaz, P. Erasenthiran, N. Hopkinson, J. Mater. Process. Tech. 195 (1-3) (2008) 77.
15. Y. Zhang, A. Faghri, J. Heat Transfer. 120 (4) (1998) 883.
16. M. Labudovic, D. Hu, R. Kovacevic, J. Mater. Sci. 38 (2003) 35.
17. A. V. Gusarov, I. Yadroitsev, Ph. Bertrand, I. Smurov, J. Heat Transfer 131 (7) (2009), 0172101-1.
18. S. Chandrasekhar, Hydrodynamic and hydromagnetic stability. Dover Publications, New York, 1981.
19. J. Mazumder, Laser-Beam Welding. In: ASM Handbook, 9th Edition, vol. 6, Welding, Brazing & Soldering, ASM International, 1983.
20. J. Mazumder, Opt. Eng. 30 (8) (1991) 1208.
21. B. J. Keene, K. C. Mills, A. Kasama, A. McLean, W. A. Miller, Metall. Mater. Trans. 17 (1) (1986) 159.
22. R. M. Digilov, J. Cryst. Growth. 249 (1-2) (2003) 363.
23. P. Fischer, V. Romano, H. P. Weber, S. Kolossov, Thin Solid Films 453-454 (2004) 139.
24. The Engineering ToolBox, www.engineeringtoolbox.com, 2005.
25. W. M. Steen, Laser Material Processing, 3rd ed. Springer, 2003.
26. M. Van Elsen, Complexity of Selective Laser Melting: a new optimisation approach. PhD thesis, Katholieke Universiteit Leuven, 2007.
27. M. Van Elsen, M. Baelmans, P. Mercelis, J.-P. Kruth, Int. J. Heat Mass Tran. 50 (23-24) (2007) 4872.
28. O. Rehme, C. Emmelmann, Proceedings of SPIE (6107) Laser-based Micropackaging, Bellingham, WA, 2006.
29. K. Maeda, T. H. Childs, J. Mater. Process. Tech. 149 (2004) 609.
30. I. Yadroitsev, Selective laser melting: Direct manufacturing of 3D-objects by selective laser melting of metal powders, Lap Lambert Acad. Publ., ISBN-978-3-8383-1794-6, 2009.
31. A. Simchi and H. Pohl, Mater. Sci. Eng. A 359 (1-2) (2003) 119.
32. X. Deng, G. Piotrowski, J. Williams, N. Chawla, Int. J. Fatig. 27 (10-12) (2005) 1233.
33. eFunda Inc., www.efunda.com, 2010.
34. G. Malygin, Phys. Solid State 49 (6) (2007) 1013.
35. F. J. Kahlen and A. Kar, J. Manuf. Sci. Eng. 123 (1) (2001) 38.
36. G. K. Lewis and E. Schlienger, Materials and Design 21 (2000) 417.
37. I. Yadroitsev, L. Thivillon, Ph. Bertrand, I. Smurov, Appl. Surf. Sci. 254 (4) (2007) 980.
38. A. H. Nickel, D. M. Barnett, F. B. Prinz, Mater. Sci. Eng. A 317 (1-2) (2001) 59.
39. M. Rombouts, Selective laser sintering/melting of iron-based powders, PhD thesis, Katholieke Universiteit Leuven, 2006.